proceedings

MDPI

Proceedings

Electromagnetic Characterization of Engineered Materials Using Capacitively Loaded Aperture Sensors †

Oleksandr Malyuskin

Queen's University Belfast, UK; o.malyuskin@qub.ac.uk

† Presented at the 6th International Electronic Conference on Sensors and Applications, 15–30 November 2019; Available online: https://ecsa-6.sciforum.net/

Published: 14 November 2019

Abstract: A novel method for electromagnetic (EM) characterization of engineered artificial materials such as bio-, nanomaterials and composite materials is proposed and experimentally evaluated in this paper. The method is based on resonance transmission properties of capacitively loaded apertures in conductive screens. The advantage of this new method over the existing techniques (free space, loaded waveguide, microstrip and coplanar waveguide resonators, coaxial probe, etc) is three-fold: i) resonance EM field enhancement inside the loaded aperture leads to very high sensitivity and therefore accuracy of EM parameters de-embedding; ii) only small thin samples of material-under test are required (with sample area substantially smaller than squared wavelength of radiation, ~0.01 λ^2); iii) the method is easily scalable over the frequency and wavelength and based on relatively simple permittivity and permeability de-embedding procedure. The experimental setup in the microwave S-band (2-3GHz) is based on two dipole antennas, capacitive aperture in the conductive screen, unloaded and loaded with material under test, and vector network analyser (VNA) for signal generation and data acquisition. Analytical de-embedding procedure is developed and applied to the characterization of carbon nanotube (CNT) material microwave absorption. It is demonstrated that the method offers very high accuracy in material characterization based on minimal material samples.

Keywords: microwave sensing**;** composite materials; electromagnetic characterization; absorption; microwave transmission; electromagnetic resonance

1. Introduction

Electromagnetic (EM) characterization of engineered artificial materials such as bio-, nanomaterials and composite materials is very important for several reasons. One of these reasons is future proliferation of 5G communication networks [1] exposing urban population into the EM radiation of wide spectral range, therefore it is critically important to understand how new materials EM response can be utilized in electronic and communication devices and also ensure the EM compatibility of biomaterials used in human body. Future smart fabrication, construction engineering, aerospace and automotive industry would also benefit from online in-situ characterization of composite materials [2] used in structures and constructions.

Microwave material characterization methods [3]-[6] are well established and can be classified into several categories, based on the microwave measurement setup: coaxial probe, transmission line, waveguide, free-space, resonant cavity or resonator and parallel plate techniques [5]-[9]. As a rule, application of these methods requires a relatively large material sample (~0.125λ^2 in waveguide-based measurement methods or >λ^2 for free space setup, λ is a wavelength of radiation) or material that can be filled inside a specific shape (e.g. resonator cavity).

In this paper we propose a new method that can be considered as a combination of free-space, parallel-plate and resonator-based methods [5]. This method allows to characterize dielectric permittivity and/or electromagnetic absorption (conductivity) and requires only a very small quantity of material (~0.0125 λ^2 or smaller cross-sectional area). The material sample could be in the form of very thin sheet (thickness ~1μm-10μm). This method can be easily scaled in the frequency/wavelength range, it features straightforward permittivity de-embedding algorithm and requires simple microwave or mm-wave measurement setup consisting of a pair of dipole antennas and capacitively loaded aperture in a conductive screen. Since the method is based on resonant microwave transmission, the signal generation and acquisition circuit topology is simple since it does not require collect reflected signal for reference. The signal chain circuit requires inexpensive electronic hardware, which makes this method very attractive for in-field automated applications.

2. Materials and Methods

2.1. Measurement Setup Geometry

The geometry of the measurement setup is shown in Fig.1. The setup consists of two dipole antennas, transmit (TX) and receive (RX), located in the near (d_{offset} ≈0.1λ-0.25λ), Fresnel (d_{offset} ≈0.25λ-0.5λ) or far field (d_{offset}>λ) zones with respect to the aperture in the conductive screen, Figure 1. Due to the differential nature of the measurement, the system will operate irrespectively of the antennas distance from the aperture.

(**a**) (**b**)

Figure 1. (**a**) Geometry of measurement setup. (**b**) Capacitive aperture loaded with carbon nanotube material in the anechoic measurement environment. .

2.2. EM Field Enhancement in the Capacitevely Loaded Aperture

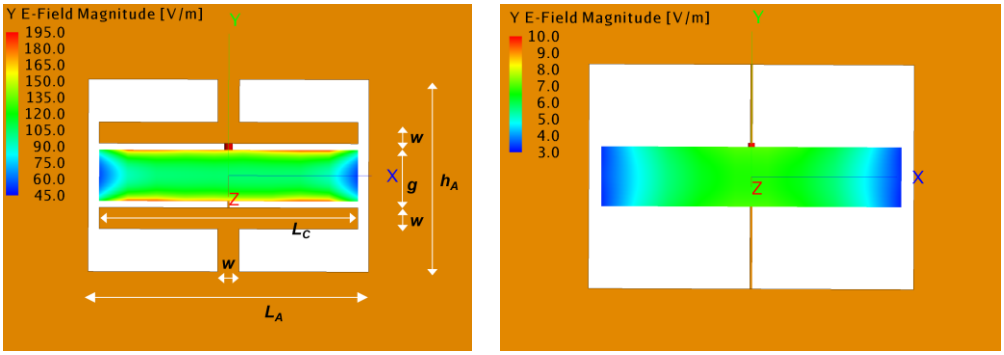

(**a**) (**b**)

Figure 2. E-field inside the capacitively loaded and unloaded apertures at transmission resonance (**a**) Ey-field magnitude inside the capacitively loaded aperture at 2.42GHz. (**b**) Ey-field magnitude in unloaded rectangular aperture at 2.176GHz.

Fig. 2(a) shows FEKO-simulated E-field enhancement inside capacitively loaded aperture designed to operate at 2.42GHz. The dimensions of the capacitively loaded aperture are L_A = 26mm, L_C = 24mm, h_A = 18mm, g=6mm, w=2mm. The unloaded rectangular aperture in Fig. 2(b) has dimensions of 26mmx18mm.

It can be seen that at the resonance, ***E-field is significantly (20 times) enhanced*** in the capacitive aperture as compared to unloaded rectangular aperture. This leads to strong EM interaction between the field in the capacitively loaded aperture and material sample under test.

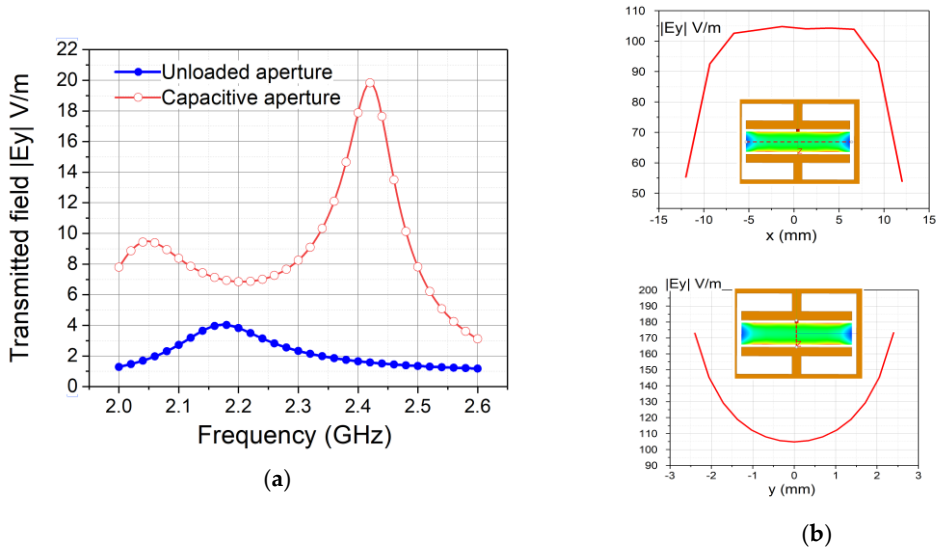

Figure 3. (**a**) Transmitted *E*y-field magnitude 10mm off the aperture on z axis (0,0,10mm). The aperture is excited by a half-wavelength y-oriented dipole antenna with the centre located at (0,0,-10mm). (**b**) Ey-field magnitude distribution inside capacitive aperture at 2.42GHz, red dashed lines show the field sampling points.

Figure 3(a) shows resonance characteristics of the transmitted field at some distance from the aperture on z axis (0,0,10mm). It can be seen that a capacitively loaded aperture leads to very strong resonance transmission as compared to the unloaded aperture case. Figure 3(b) shows dominant Ey-field component inside the aperture "capacitor". It is interesting to note that while the Ey-field is uniform along x, it changes parabolically along the vertical y direction.

2.3. Material Sample Permitivity and EM Loss Characterization Using Equivalent Circuit Model

In order to develop EM parameters de-embedding procedure, let us consider the equivalent circuit model of the capacitively loaded aperture with and without the material sample, Figure 4.

In Figure 4 the equivalent lump parameters are given by the EM relations [10,12]

Unloaded aperture capacitance C_0 and inductance L_0 are given by expressions

$$\frac{1}{C_0} = \frac{1}{4\pi\varepsilon_0 |q_0|^2} \iint_{Sg} \frac{\rho(\boldsymbol{r})\rho(\boldsymbol{r}')}{|\boldsymbol{r}-\boldsymbol{r}|} d\boldsymbol{r}d\boldsymbol{r}' \tag{1}$$

$$L_0 = \frac{\iint_{Sg} \boldsymbol{H}\cdot\boldsymbol{r}drdr'}{\langle I_0 \rangle} \tag{2}$$

Where q_0 and I_0 are maximum charge across the aperture "capacitor" plates and average maximum current delivered to the aperture "capacitor". Z_{FS} is a characteristic impedance,

$$Z_{FS} = Ey/Hx \tag{3}$$

In general, Z_{FS} is a complex number if the TX/RX antennas are located in the near or Fresnel field zone. In (1), (2), the integration is carried out over the Sg "capacitive gap" area shown in Figure 2(a).

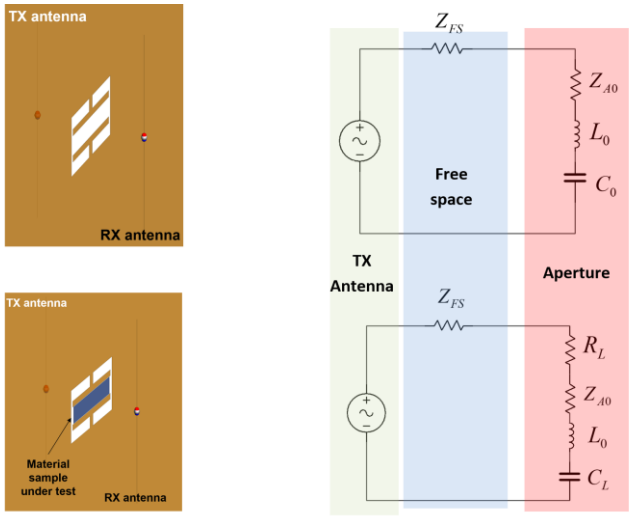

Figure 4. Equivalent electric lumped-element circuits of capacitive aperture, unloaded and loaded with material sample.

Consider the situation, when the capacitive aperture is loaded with thin dielectric material which does not lead to the change in the aperture self-inductance. Next, assuming that the *E*-field is approximately uniform inside the capacitive gap (more accurate study taking into account spatial field variation, Fig.3b will be reported in full paper) one can write the resonance frequencies of empty and sample-loaded capacitive aperture as

$$f_{res}^{(0)} = \frac{1}{2\pi\sqrt{L_0 C_0}} \qquad f_{res}^{(L)} = \frac{1}{2\pi\sqrt{\kappa' L_0 C_0}} \tag{4}$$

Where the real part κ' of the material wavenumber $\kappa = \sqrt{\varepsilon}$, ε is a complex permittivity of material. From (4), the real part of the material wavenumber can be found as

$$\kappa' = \left[f_{res}^{(0)} / f_{res}^{(L)}\right]^2 \tag{5}$$

To characterize EM loss due to material, it is possible to estimate the quality factor of the resonance transmission (transmitted E-field or power vs frequency *f*) of loaded and unloaded apertures. Taking into account that the power loss due to dielectric loss in capacitor can be represented as

$$P_L = V^2 \omega C_0 \kappa'' \tag{6}$$

Where κ'' is an imaginary part of wavenumber in material, the additional resistance due to material load in circuit Fig.4 can be written as

$$R_L = \left(1/2\pi f C_0 \kappa''\right) \tag{7}$$

Finally, combining (4)-(7) one can get expression for κ'' in terms of quality factors of unloaded and loaded aperture transmission characteristics (transmitted power vs frequency),
$Q_0 = 1/\omega_0 R C_0, Q_L = 1/\omega_L R_L C_L$,

$$\kappa'' = \left[\frac{1}{Q_L \sqrt{\kappa'}} - \frac{1}{Q_0} \right]^{-1} \tag{7}$$

3. Experimental Results and Discussion

Initial experimental results are presented in Figure 5 for the case of carbon nanotube (CNT) material. There are several interesting observations that can be made.

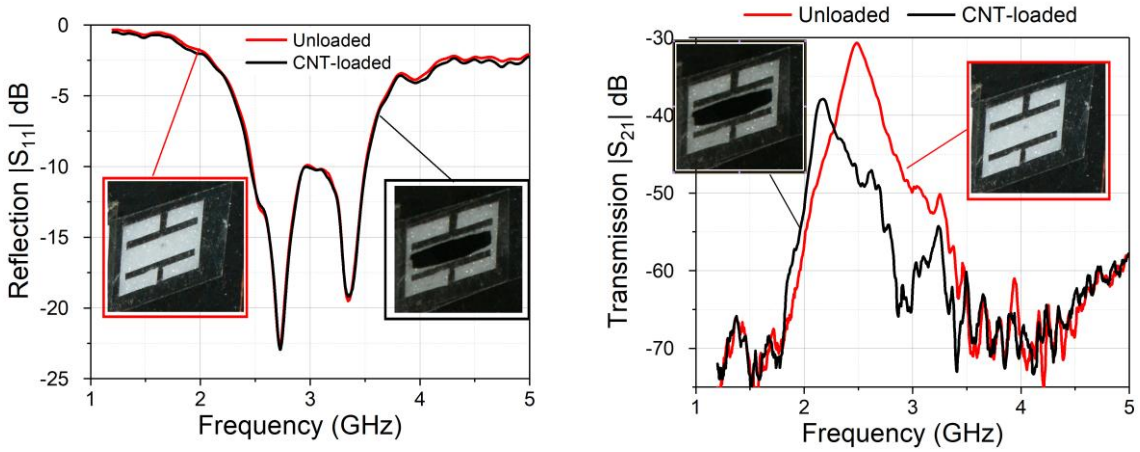

(**a**) (**b**)

Figure 5. (**a**) Reflection parameter magnitude |S11|of the loaded and unloaded apertures in the S-band. (**b**) Transmission parameter |S21|, the aperture has dimensions L_A = 26mm, L_C = 24mm, h_A = 18mm, g=6mm, w=2mm.

First, it can be clearly seen, Figure 5(a), that the aperture operates in reflection-less regime, when all the radiation from a TX antenna is transmitted through. This simplifies the analysis and de-embedding of material parameters. It is possible to apply approximate formulas (4)-(7) to extract material parameters of the CNT material from the transmission data, Fig.5(b). The results are summarized in the Table 1.

Table 1. This is a table. Tables should be placed in the main text near to the first time they are cited.

$f_{res}^{(0)}$	Q_0	$f_{res}^{(L)}$	Q_L	κ'	κ''
2.485GHz	14.2	2.170GHz	11.4	1.31	160.8

The data in Table 1 show that the CNT material introduces high loss at 2-3GHz range with very moderate value of the real part of wavenumber κ'.

The e-embedding procedure proposed here is based on approximation of capacitively loaded aperture as a high-frequency capacitor with subsequent use of low-frequency formulas for the resonance frequency shift and quality factors of a loaded capacitor. More accurate de-embedding procedure based on full wave EM field calculations will be reported elsewhere in future.

Acknowledgments: The author is thankful to Prof. Davide Mariotti and Dr Paul Brunet for providing CNT material samples and helpful discussions.

Conflicts of Interest: "The author declares no conflict of interest."

References

1. Yang, P.; Xiao, M. and Li, S.; 6G Wireless Communications: Vision and Potential Techniques. *IEEE Network*, **2019**, *33*, 70–75.

2. Kharkovsky S., Zoughi R. Microwave and millimeter wave nondestructive testing and evaluation - Overview and recent advances. *IEEE Instrum. Meas. Mag.* **2007**, *10*, 26–38.
3. Kaatze, U. Techniques for measuring the microwave dielectric properties of materials. *Metrologia*, **2010**, *47*, S91–S113.
4. Brodie, G.; Jackob, M.; Ferrell. P. 6 Techniques for Measuring Dielectric Properties. In *Microwave and Radio-Frequency Technologies in Agriculture*, Sciendo: Berlin, Germany.
5. Basics of Measuring the Dielectric Properties of Materials, Keysight. Available online: http://literature.cdn.keysight.com/litweb/pdf/5989-2589EN.pdf (accessed on 21 October 2019).
6. Baker-Jarvis J.; Janezic, M.; Degroot D.; High-Frequency Dielectric Measurements. Part 24 in a Series of Tutorials on Instrumentation and Measurement. *IEEE Instrum. Meas. Mag.* **2010**, *13*, 24–31.
7. Akhtar, M.J.; Feher, L.E.; Thumm. M. A closed-form solution for reconstruction of permittivity of dielectric slabs placed at the center of a rectangular waveguide. *IEEE Geosci. Remote Sens. Lett*., **2007**, *4*, 122–126.
8. Mirzavand, R. Honari, M. M., Mousavi, P. High-Resolution Dielectric Sensor Based on Injection-Locked Oscillators. *IEEE Sensors J.* **2018**, *18*, 141–148.
9. Vlachogiannakis, G., Hu, Z., Shivamurthy, H. T., Neto, A., Pertijs, M. A., de Vreede, L. C., Spirito, M. Miniaturized Broadband Microwave Permittivity Sensing for Biomedical Applications. *IEEE J. Electromagntics, RF Microw. Med. Biol.* **2019**, *3*, 48.
10. Butler, C.; Rahmat-Samii, Y.; Mittra, R. Electromagnetic penetration through apertures in conductive surfaces. *IEEE Trans. Antennas Propagat*. **1978**, *EMC-20*, 82–93.
11. Malyuskin O., Fusco, V.; High-Resolution Microwave Near-Field Surface Imaging Using Resonance Probes, *IEEE Trans. Instrum. Meas*. **2016**, *36*, 189–200.
12. Balanis, C.; Antenna Theory: Analysis and Design, John wiley & sons: Hoboken, NJ, USA, 2016.
13. Nozokido,T.; Miyasaka, N.; and Bae,J.; Near-field slit probe incorporating a micromachined silicon chip for millimeter-wave microscopy. *Microw. Opt. Technol. Lett*. **2011**, *53*, 660–664.
14. Vykhodtsev, A.; Kordi B.; and Oliver,D.; Sensitivity analysis of a parallel-plate method for measuring the dielectric permittivity of high-voltage insulating materials. *High Voltage* **2017**, *2*, 200–204.